Published in final edited form as:
*Biochim Biophys Acta*. 2011 December ; 1814(12): 1748–1757. doi:10.1016/j.bbapap.2011.09.010.

# Elongin C is a Mediator of Notch4 Activity in Human Renal Tubule Cells

**Timothy D. Cummins**[1], **Michael D. Mendenhall**[3], **Michelle N. Lowry**[2], **Erik A. Korte**[1], **Michelle T. Barati**[2], **Syed J. Khundmiri**[2], **Sarah A. Salyer**[2], **Jon B. Klein**[1,2], and **David W. Powell**[1,2,*]

[1]Departments of Biochemistry and Molecular Biology, University of Louisville School of Medicine

[2]Department of Medicine, University of Louisville School of Medicine

[3]Department of Molecular & Cellular Biochemistry, University of Kentucky

## Abstract

Notch proteins (Notch 1–4) are a family of trans-membrane cell surface receptors that are converted into transcriptional regulators when activated by interactions with cell surface ligands on adjacent cells. Ligand-binding stimulates proteolytic cleavage of the trans-membrane domain, releasing an active intracellular domain (ICD) that translocates to the nucleus and impacts transcription. In transit, the ICD may interact with regulatory proteins that modulate the expression and transcriptional activity. We have found that Notch4$^{ICD}$ expression is enhanced in the tubule cells of fibrotic kidneys from diabetic mice and humans and identified Notch4$^{ICD}$ interacting proteins that could be pertinent to normal and pathological functions. Using proteomic techniques, several components of the Elongin C complex were identified as candidate Notch4$^{ICD}$ interactors. Elongin C complexes can function as ubiquitin ligases capable of regulating proteasomal degradation of specific protein substrates. Our studies indicate that ectopic Elongin C expression stimulates Notch4$^{ICD}$ degradation and inhibits its transcriptional activity in human kidney tubule HK11 cells. Blocking Elongin C mediated degradation by MG132 indicates the potential for ubiquitin-mediated Elongin C regulation of Notch4$^{ICD}$. Functional interaction of Notch4$^{ICD}$ and Elongin C provides novel insight into regulation of Notch signaling in epithelial cell biology and disease.

## Introduction

Notch family proteins are single-pass trans-membrane receptors that regulate cell fate decisions in a variety of developmental processes including neurogenesis, myogenesis, vasculogenesis, hematopoiesis, and skin and kidney development [1–6]. The four mammalian Notch isoforms share a common general structure consisting of an extracellular domain comprised chiefly of up to 34 tandem epidermal growth factor-like (EGF-like) repeats and 3 tandem Notch-homology repeats; a trans-membrane domain; and an intracellular domain (ICD) consisting of a RAM domain that interacts with the RBP-Jk transcriptional complex, multiple tandem ankyrin repeats, a spacer region and a carboxy



Address Correspondence to david.powell@louisville.edu, 570 South Preston St., Baxter Research Building I, Room 204D, Louisville, KY 40202 Phone: 502-852-5239, Fax: 502-852-4384.



The authors indicate no declaration of financial interests.

terminal PEST region [7]. In the canonical Notch pathway, the binding of ligand (jagged or delta-like-ligand isoforms), which is usually expressed on the surface of a contacting cell, to the extracellular domain of Notch initiates a series of proteolytic events in and near the transmembrane domain that releases the ICD from its membrane attachment [8]. The Notch$^{ICD}$ is translocated to the nucleus where it displaces co-repressors and assembles transcriptionally active complexes containing CSL (CBF-1/RBP-Jk in vertebrates, Suppressor of hairless in *Drosophila*, and LAG-1 in *C. elegans*) elements on specific promoters, and excludes histone deacetylase (HDAC) proteins [9]. The nature of the target genes and the degree to which they are activated determine the subsequent fate of the signal conveyed by the Notch receptors [10].

We are interested in defining molecular events that contribute to diabetic kidney disease or nephropathy, the leading cause of end-stage-renal disease (ESRD) in the Western World. Tubulointerstitial fibrosis (TIF) correlates with the degree of renal dysfunction and appears to be critical in the progression of diabetic nephropathy to ESRD [11, 12]. The link between aberrant transforming growth factor-β (TGF-β) signaling and TIF is particularly compelling in diabetic nephropathy [13]. Previous reports indicate a role for Notch4 activity in TGF-β function in epithelial-derived breast tumor, smooth muscle, and endothelial cell lines [14–16]. We show here that over-expression of the active Notch4$^{ICD}$ augments TGF-β fibrotic activity in a human-derived kidney tubule (HK11) cell line, suggesting that perhaps Notch4 activity is elevated in tubule cells under fibrotic conditions in diabetic nephropathy. In support of this postulation we have found that tubule Notch4$^{ICD}$ expression is enhanced in fibrotic kidneys from diabetic mice and humans.

To define proteins that regulate Notch4$^{ICD}$ function and that may play a role in TGF-β signaling in kidney disease, we initiated a proteomic analysis of Notch4$^{ICD}$ interactors in HK11 renal proximal tubule cells. Our studies identified Elongin C as a candidate interactor. Elongin C, a 13 kDa protein also named transcription elongation polypeptide B1 (TCEB1), has two described biochemical functions. As part of a complex with Elongin A and Elongin B, it regulates transcription via direct interaction with RNA polymerase II, in fact Elongin C acts in concert with another ubiquitin ligase, Rsp5 (human homologue NEDD4) and Elongin A to eventually polyububiquitinate RNA pol II in response to DNA damage [17, 18]. As part of a family of separate complexes containing Elongin B and various substrate specificity factors, it acts as an E3 ubiquitin ligase [19, 20]. A role in Notch1 signaling has been described for a different E3 that uses the F box protein Fbw7/Sel-10 as the substrate receptor for a cullin-1-based ubiquitin ligase activity [21, 22]. Fbw7/Sel-10 has been shown to bind phosphorylated Notch1$^{ICD}$ and Notch4$^{ICD}$ *in vitro* [22]. However, although Fbw7/Sel-10 over-expression depressed Notch1 activity and protein levels, no effect of Fbw7/Sel-10 over-expression was seen on Notch4 expression or signaling. Notch upregulates the transcription of the Ankyrin-SOCS binding genes generating Asb proteins that appear to be more responsible for targeting Notch substrates such as E2A and Jak2 [24]. This and an earlier report [25] show that Asb2 utilize an Elongin B/C Cullin complex to target E2A and Jak2 substrates, but no data have shown Notch to be targeted by such complexes. This prompted us to explore the possibility that Notch4 was regulated by Elongin C via an ubiquitin ligase process. We find that Elongin C associates with Notch4$^{ICD}$ and plays a role in its function through regulation of protein stabilization in a proteasome-dependent manner.

## Materials and Methods

### Animal Studies

Were performed with transgenic OVE26 type 1 diabetic and FVB background control strain mice (Jackson Laboratory, Bar Harbor, Maine). All animal procedures adhered to the guidelines of the National Institutes of Health Guide for the Care and Use of Laboratory

Animals and were approved by the University of Louisville Institutional Animal Care and Use Committee. There was also Internal Review Board approval for immunostaining of archived kidney biopsy sections from diabetic and normal individuals.

## Notch Constructs

All constructs used the intracellular domain (ICD) of human Notch4. The initial clone was purchased from GenScript Corp. (Piscataway, NJ) as a synthetic construct flanked by convenient restriction sites in pUC57. DNA sequencing confirmed that the synthetic construct encoded a polypeptide identical to residues 1467 to 2003 of the reference sequence for human Notch4 (GenBank NP 004538.3). All subsequent constructs were generated by direct sub-cloning from this parent into appropriate expression vectors. For protein isolation for mass spectrometry, a derivative of pcDNA3-CTAP (gift of Anne-Claude Gingras, Samuel Lunenfeld Research Institute [26]) was used. The multiple cloning site (MCS) was altered to accept an *Xho*I-*Bam*HI fragment. pcDNA3-CTAP adds a sequence encoding a calmodulin-binding domain, a tobacco etch virus (TEV) protease site and the IgG-binding domain of *S. aureus* protein A to the carboxy terminus of the insert and utilizes a CMV promoter for transcription. Carboxy-terminal fusion tags consisting of the fluorescent markers, GFP and ZsYellow1 were added by cloning into MCS-altered derivatives of pGFP-N1 and pZsYellow1-N1 purchased from Clontech (Mountain View, CA). V5 epitope was added to the carboxy terminus using synthetic oligonucleotide linkers.

## Elongin C Constructs

All constructs were ultimately derived from clone SC116611 purchased from Origene (Rockville, MD). Convenient restriction sites were added 5’ and 3’ to the coding region by PCR allowing cloning into vectors to produce FLAG-ElgC, Cyan1-ElgC, GFP-ElgC and V5-ElgC. The insert was sequenced and matched to the reference sequence for human Elongin C (GenBank NM 005648.2).

## Transfections

All transfections were done with immortalized proximal tubule-derived human kidney (HK11) cells (gift from Dr. Lorraine Racusen, Johns Hopkins University), at a ratio of 4:2 (μl reagent (Fugene HD, Roche, Indianapolis, IN): μg DNA) overnight in OPTI-MEM low serum (0.5% FBS) medium.

## Lysate Preparation

Transfected cells were washed 3X with cold PBS and then lysed in TAP lysis buffer (10% glycerol, 50 mM HEPES-KOH (pH-8.0), 100 mM KCl, 2 mM EDTA, 0.1% NP-40, 2 mM DTT, 10 mM NaF, 0.25 mM NaF, 0.25 $Na_3VO_4$, 5 nM okadaic acid, 5 nM calyculin, 50 mMβ-glycerolphosphate, 1:100 protease Inhbitor Cocktail from Sigma-Aldrich P2714) for 30 min. at 4°C. The lysate was clarified by centrifugation for 30 minutes, 20,000 × g at 4°C.

## Immunoblot

Proteins were separated by 4–15% gradient SDS-PAGE and transferred to nitrocellulose membranes using the Biorad system (Hercules, CA). Immunoblotting was performed using our previously reported method [27]. Primary antibodies included those reactive to $Notch4^{ICD}$ (Millipore, Billerica, MA, Cat. # 07–189), V5 epitope (Invitrogen, San Diego. CA), GAPDH (Millipore), Elongin C (Biolegend, San Diego, CA, Cat. # 613102), GFP (Roche, Indianapolis, IN, Cat. # 11814460001), Fibronectin (Santa Cruz Biotech., Santa Cruz, CA, Cat. # Sc-8422) and RNA polymerase II (Cell Signaling, Cat. # 2629).

### Immunopurification

HK11 cells were lysed in RIPA buffer with protease inhibitors. 1mg lysate (2X) was pre-cleared with 10 µl Protein A Sepharose beads for 1 hour at 4°C. Then the supernatant was removed for overnight incubation at 4°C with 10 µl Protein A Sepharose beads alone (control) or 10 µl Protein A Sepharose beads plus 4 µg Polyclonal anti-Notch4 (Millipore, Cat. # 07–189). Next, lysate was removed and the beads were washed 3 times with 1 ml PBS. Protein complexes were eluted with SDS sample dilution buffer, separated by 4–20% SDS-PAGE, and transferred to nitrocellulose membrane. Nitrocellulose membrane was cut into the desired molecular weight ranges and probed with either 1µg/ml of the same polyclonal Notch4 antibody or 0.2 1µg/ml polyclonal anti-Elongin C (Biolegend, Cat. # 613102). 50 µg HK11 lysate was probed for Elg C and Notch4$^{ICD}$ using the same antibodies to determine their relative concentration or input.

### Immunohistochemistry

Experiments were performed with human kidney biopsy sections as previously described [27]. Primary antibodies included those reactive to Notch4$^{ICD}$ (Millipore, Billerica, MA), Elongin C (Biolegend, San Diego, CA), and TGF-β (Santa Cruz Biotech., Santa Cruz, CA).

### Tandem Affinity Purification

HK11 cells were plated to ~80% confluence. Ten (10 cm) cell culture dishes were transiently transfected with 5 µg of plasmid TAP-Notch4$^{ICD}$ for ~48 hours. Cells were washed 3 times in ice cold PBS then scraped and pelleted. Resulting cells were lysed in 2 mL TAP lysis buffer on ice for 30 min with repeated sonication. The lysate was clarified by centrifugation for 30 minuntes, 20,000 × g at 4°C. Lysate was pre-cleared in Sepharose beads for 30 min prior to TAP isolation procedure. Approximately 50 mg total protein extract in lysis buffer was added to ~100 µL of pre-washed covalently linked IgG-Sepharose beads (GE healthcare Bio-Sciences, Uppsala, Sweden) and placed on a rocker for 4 hrs at 4°C. Beads were collected and washed 3X in 10 volumes TAP lysis buffer then washed and resuspended in 10 volumes Tobacco Etch Virus (TEV) digestion buffer (10 mM HEPES-KOH (pH 8.0), 150 mM NaCl, 0.5 mM EDTA, 0.1% NP-40, 1 mM DTT). TEV protease was incubated at 100 U/100 µL IgG-Sepharose beads at 4°C with 200 RPM agitation for 4 hours. Supernatant was collected and diluted into 1 volume of calmodulin binding buffer (10 mM mercaptoethanol, HEPE-KOH pH 8.0, 150 mM NaCl, 1mM MgOAc, 1 mM imidazole, 0.1% NP-40, 2 mM $CaCl_2$) with ~100 µL calmodulin sepharose beads for 90 minutes on a rocker at 4°C. Beads were washed 3X with fresh calmodulin binding buffer and 2X with calmodulin rinsing buffer (50 mM Ammonium bicarbonate pH 8.0, 75 mM NaCl, 1mM MgOAc, 1 mM imidazole, 2 mM $CaCl_2$). Cleaved Notch4$^{ICD}$ was then eluted in 50 mM ammonium bicarbonate and 25 mM EGTA. Resulting elution was protease digested with purified porcine trypsin (Promega, Madison, WI.) and peptides were captured on a reversed phase C18 trap column, washed, then eluted into 95% HPLC grade acetonitrile. Acetonitrile was vacuum centrifuged and lyophilized peptides were resuspended in 0.05% formic acid, 5% acetonitrile for 2D-LC-MS/MS analysis.

### Mass Spectrometry

Notch4$^{ICD}$ complexes were analyzed with a Thermo LTQ linear ion trap using a previously described 2D-LC-MS/MS approach [27]. Database searching was performed with tandem mass spectra extracted by ReadW and converted to mzXML format. Charge state deconvolution and deisotoping were not performed. All MS/MS samples were analyzed using SequestSorcerer (Sage-N, Milpitas, CA). Sequest was set up to search a FASTA-formatted human protein database (Human RefSeq, 2007). Searches were performed with a fragment ion mass tolerance of 1.00 Da and a parent ion tolerance of 1.2 Da. Iodoacetamide

derivative of cysteine was specified as a fixed modification. Oxidation of methionine was specified as a variable modification.

Scaffold (version Scaffold 3.0.00, Proteome Software Inc., Portland, OR) was used to validate MS/MS based peptide and protein identifications. Peptide identifications were accepted if they could be established at greater than 95.0% probability as specified by the Peptide Prophet algorithm [28]. Protein probabilities were assigned by the Protein Prophet algorithm [29]. Protein identifications were accepted if they could be established at greater than 95.0% probability. Proteins that contained similar peptides but could not be differentiated based on MS/MS analysis alone were grouped to satisfy the principles of parsimony.

## Luciferase Assays

Rbp-Jk and SMAD 2/3/4 luciferase reporter assays (SAbiosciences, Frederick, MD) were performed in the presence or absence of appropriate Notch4$^{ICD}$, Elongin C, or control vectors. Transfections were supplemented with control vectors to equalize any difference in total plasmid concentration. HK11 cells were transfected with a Rbp-Jk or SMAD responsive firefly luciferase construct and constitutively expressing *Renilla* luciferase construct (at 40:1 ratio) using Fugene HD (Roche, Madison, WI) at an optimized 4:2 μl Fugene HD/μg DNA ratio. Cells were incubated in reduced serum OPTIMEM medium (Gibco, Carlsbad, CA) at 37°C, 5% $CO_2$ for 24–48 hours then harvested by passive lysis extraction for 30 minutes at room temperature on a shaker. Approximately 20% of the lysate was loaded into designated wells of a 96 well plate for measurement in a luminometer (Perkin Elmer Victor3, Waltham, MA). Each well was injected with 50 μl of luciferase substrate and immediately injected with quenching reagent and *Renilla* substrate and luminescence was measured. Acquired data were expressed as a ratio of firefly luminescence to renilla luminescence and normalized to vector control samples or Notch4$^{ICD}$ response where appropriate.

## Confocal Microscopy

HK11 cells were seeded at ~2 × $10^4$ cells/chamber overnight then transfected using Fugene HD at an optimized 4:2 μl/μg HD/DNA ratio overnight with Notch4$^{ICD}$-GFP, ElgC-GFP or GFP as control. Images were acquired on an Olympus FLUOVIEW FV1000 microscope (Center Valley, PA) and processed in a manner similar to our previous report [27]. GFP was excited at 488 nm and images were captured with Kalman frame setting at 10 frames and 5–10 pixel/μs resolution.

## FRET Image Analysis

For CYFRET imaging experiments in living cells, HK11 cells were transfected with CFP-Elongin C and YFP-Notch4$^{ICD}$ for 24–48 h and then viewed and analyzed with an Olympus FRET/TIRF microscope (Center Valley, PA). CYFRET image acquisition and analysis was done using SlideBook software. The software is based on the three-filter "micro-FRET" image subtraction method described by Jiang and Sorkin [30]. Briefly, three images (100-ms or 250-ms exposure sets, 2 × 2 binning) were obtained: a YFP excitation/YFP emission image; a CFP excitation/CFP emission image; and a CFP excitation/YFP emission image (raw, uncorrected CYFRET). After imaging, background images were taken. Background-subtracted YFP and CFP images were fractionally subtracted from raw CYFRET images based on measurements for CFP bleed-through (0.50–0.56) and YFP cross-excitation (0.015–0.02). This fractional subtraction generates corrected FRET$^C$ images. The corrected images were represented in pseudo-color (gated to YFP acceptor levels), showing sensitized FRET within cells. The subtraction Pearson's coefficients were rounded up from average cross-bleed values determined in cells expressing CFP- or YFP-tagged constructs alone.

Thus, these coefficients result in the underestimation of $FRET^C$ signals for true FRET partners but prevent false positive detection of FRET.

### Quantitative Real-Time RT-PCR

HK11 cells were transfected with appropriate plasmid constructs, then lysed and RNA extracted using SAbiosciences qPCR grade RNA isolation kit. RNA was quantified and ~50 ng was converted to cDNA by reverse transcription and qPCR was performed using appropriate primers for Fibronectin, Notch1, Notch4 or Elongin C and 18S rRNA (obtained from SAbiosciences) with the ABI-7500 qPCR thermal cycler and $qRT^2$-PCR SYBR/ROX master mix per manufacturer's protocol (Qiagen Valencia, CA.). 18S rRNA was used to normalize $C_t$ for all genes.

## Results

### $Notch4^{ICD}$-mediated TGF-β activity and expression of $Notch4^{ICD}$ in fibrotic kidneys

Defining novel regulators of the pro-fibrotic activity of TGF-β in diabetic kidney disease is critical towards understanding the molecular basis of this disease process. Previous reports indicate a role for Notch4 activity in TGF-β function in epithelial-derived breast tumor, smooth muscle, and endothelial cell lines [14–16]. Thus, we investigated whether over-expression of the active $Notch4^{ICD}$ would affect TGF-β transcription and fibrotic activity in a human proximal tubule HK11 cell line. TGF-β SMAD-directed transcription responses were measured in HK11 cells transfected with a SMAD2/3/4 luciferase reporter with and without co-transfection of $Notch4^{ICD}$ overnight and then treated with TGF-β for 24 hours. Although having no effect by itself, $Notch4^{ICD}$ potentiated TGF-β -stimulated SMAD2/3/4 transcriptional activity in this assay (Figure 1A). Figure 1B shows that fibronectin protein levels, a marker for TGF-β induced fibrosis, also increased relative to what is seen with TGF-βalone when $Notch4^{ICD}$ was ectopically expressedWe also found that $Notch4^{ICD}$ over-expression augments TGF-β-directed transcription of PAI-1, a gene that contains SMAD3/4 binding elements, and the gene for extracellular matrix protein fibronectin in human-derived kidney tubule HK11 cells (Figure 1C). PAI-1 is also a well-recognized pro-fibrotic gene. These findings represent $Notch4^{ICD}$ activation of SMAD-dependent TGF-β signaling. Figure 1D shows that the $Notch4^{ICD}$-GFP construct used in these TGF-β activity experiments is transcriptionally active in HK11 cells.

These findings suggested that perhaps Notch4 activity is accelerated in tubule cells under fibrotic conditions in chronic kidney disease. To test this postulation, $Notch4^{ICD}$ levels were measured in fibrotic kidneys from transgenic OVE26 type 1 diabetic mice and type 1 diabetic patients. Figure 2A shows that a specific $Notch4^{ICD}$ band is elevated in 3 out of 4 whole kidney extracts from OVE26 mice as compared with samples from background control strain. Each sample was prepared from a pool of kidney extract from 4 different mice, effectively measuring 16 animals for $Notch4^{ICD}$ protein levels. Fibrotic features for each kidney sample was confirmed by Mason's trichrome staining (Zheng and Epstein unpublished results). Immunohistochemistry (IHC) in Figure 2B further shows that $Notch4^{ICD}$ expression is enhanced in tubule cells of kidney biopsies from type 1 diabetic patients with tubulointerstitial fibrosis as indicated by blue collagen staining with Mason's trichrome. Evident is mostly diffuse cellular expression of the $Notch4^{ICD}$ (solid arrows) with some cells showing enriched nuclear expression (dashed arrows), a consistent localization pattern for active $Notch4^{ICD}$. Tubular TGF-β levels were also elevated in the human diabetic kidney sections (Figure 2C). Together, this suggests a role for over-activation of Notch4 in kidney fibrogenesis in diabetes.

### Identification of Elongin C as a candidate Notch4$^{ICD}$ interactor

To define proteins that regulate Notch4$^{ICD}$ expression levels and that may function in TGF-β signaling in kidney biology and disease, we initiated a proteomic analysis of Notch4$^{ICD}$ interactors in HK11 cells. For this, the intracellular domain of human Notch4, starting at the putative γ-secretase cleavage site (S3) that releases Notch4$^{ICD}$ from the membrane (aa$^{1467}$ to aa$^{2003}$, [31]) was fused in-frame with a carboxy terminal TAP tag provided by pcDNA3-CTAP [26]. The TAP tag purification (TAP) construct consists of a single calmodulin-binding and IgG-binding domains separated by a TEV protease cleavage site. Notch4$^{ICD}$ complexes isolated in this manner were then digested with trypsin and the resulting peptides fractionated and identified by 2D-LC-MS/MS. Analyses of four independent Notch4$^{ICD}$ preparations were compared to that of two other unrelated target proteins as controls and the TAP tag purified with no fusion. We found that Elongin C was enriched in all Notch4$^{ICD}$ samples, but was not present in control isolates. Interestingly, a number of previously characterized members of Elongin C complexes were also identified in one or more Notch4$^{ICD}$ isolations (Table 1). This prompted a further investigation of the functional consequences of the interaction between Notch4$^{ICD}$ and Elongin C.

### Elongin C regulates Notch4$^{ICD}$ function and protein levels

The physical association between Elongin C and Notch4$^{ICD}$ indicated by the mass spectrometry results was confirmed in intact HK11 cells with fluorescence resonance energy transfer (FRET) (Figure 3A). Notch4$^{ICD}$ and Elongin C were tagged at their carboxy termini with yellow fluorescent protein (YFP) and N-termin with cyan fluorescent protein (CFP), respectively. The Notch4$^{ICD}$-YFP localized to numerous punctate spots within the nucleus of the HK11 cells. CFP-Elongin C was found primarily in the cytoplasm and less in the nucleus. In cells co-transfected with both fusion proteins, a robust FRET signal was seen with emission emanating from several punctate spots in the nucleus and some apparently cytoplasmic regions, indicating that a sub-fraction of the total cellular pool of Elongin C interacts with Notch4$^{ICD}$. This interaction is further supported by the results in Figure 3B showing that endogenous Elongin C and Notch4$^{ICD}$ co-purify from HK11 lysates.

To ascertain whether there is a functional consequence to the Elongin C-Notch4$^{ICD}$ interaction, we tested the effect of elevated Elongin C expression on Notch4$^{ICD}$-directed transcription using luciferase reporter assays. HK11 cells co-transfected with Elongin C and Notch4$^{ICD}$ stimulated transcription from a Notch responsive Rbp-Jk luciferase reporter significantly less well (~40%) than did cells transfected with Notch4$^{ICD}$ alone (Figure 3C.), indicating a potential inhibitory role for Elongin C in Notch4$^{ICD}$ function.

### Determination of Elongin C effects on Notch4$^{ICD}$ protein stability

Since Elongin C is a component of an E3 ubiquitin ligase complex and other components of this complex co-purified with the Notch4$^{ICD}$ (Table 1), we examined whether Elongin C inhibition of Notch4 transcription activity is mediated by proteasome activity. For this, the luciferase reporter assay shown in Figure 3B was conducted with and without the proteasome inhibitor MG132 (25 μM pretreatment). The inhibitory effect on Notch4$^{ICD}$ activity was attenuated in the presence of the proteasome inhibitor (Figure 4A). We next determined if over-expression of Elongin C had an impact on Notch4$^{ICD}$ protein stability. HK11 cells co-transfected with V5-Notch4$^{ICD}$ and V5-Elongin C expressed substantially lower levels of Notch4$^{ICD}$ protein than did cells transfected with Notch4$^{ICD}$ alone (Figure 4B lanes 3–4 versus 5–6), also note expression of GFP-Notch4$^{ICD}$ is diminished in HK cells when co-expressed with GFP-ElgC (lower panel Figure 4B). The extent of Elongin C-mediated reduction in Notch4$^{ICD}$ protein is also similar to that for the transcriptional activity shown in Figure 3B and 4A. Figure 4C shows that different Notch4$^{ICD}$ fusions behaved similar in the presence of ectopic Elongin C while MG132 pretreatment stabilizes

Notch4$^{ICD}$ protein levels. This is consistent with the effect of MG132 treatment on Elongin C inhibition of Notch4$^{ICD}$-directed transcription activity shown in Figure 4A and together suggests a role for Elongin C in the stimulation of Notch4$^{ICD}$ polyubiquitination and subsequent degradation by the 26S proteasome. Interestingly, there also appears to be diminished levels of Elongin C in the presence of over-expressed Notch4$^{ICD}$ (Figure 4B, confocal and immunoblot), suggesting a reciprocal functional interaction where Elongin C may be degraded after ubiquitination of this substrate. As further support of Elongin C regulation of Notch4$^{ICD}$ protein and activity through a proteasome-mediated mechanism, ectopic expression of Elongin C in HK11 cells had no effect of Notch4 or Notch1 (control) mRNA levels while Elongin C mRNA is increased in GFP-ElgC transfected cells (Figure 4D).

### Elongin C regulates Notch4$^{ICD}$-mediated TGF-β fibrotic activity

We demonstrate in Figure 1B that over-expression of Notch4$^{ICD}$ augments TGF-β-induction of fibronectin in HK11 cells. Figure 5A illustrates that co-expression with Elongin C rendered Notch4$^{ICD}$ less efficient at synergistically up-regulating the TGF-β response. Ectopic expression of GFP-tagged Notch4$^{ICD}$ and Elongin C was confirmed by immunoblot with anti-GFP and anti-Notch4$^{ICD}$ antibodies. Consistent with the results in Figure 4B co-expression with Elongin C resulted in diminished Notch4$^{ICD}$ expression and vice versa. RNA polymerase II levels were not affected by over-expression of Elongin C, further suggesting that the effects of Elongin C on Notch4$^{ICD}$ are not due to alteration of the transcriptional machinery, but rather are at the level of the Notch4$^{ICD}$ protein. Together these results suggest that Elongin C plays a role in the control of Notch4$^{ICD}$ protein levels in normal and pathological states of kidney proximal tubule cells. In support of a dysfunction of Elongin C in the regulation of Notch4$^{ICD}$ in diabetic kidney disease, immunoblot of type 1 diabetic mouse tubule extracts and immunohistochemical analysis of biopsies from type 1 diabetic patients with tubulointerstitial fibrosis show diminished tubule Elongin C levels (Figure 5B).

## Discussion

TGF-β is a major signaling effector in the progression of diabetic kidney disease and fibrosis. Multiple other signaling effectors feed into and provide cross-talk modulation of the initial TGF-β stimulus, including Akt/PKB, MAPKs (p38, Erk and Jnk) as well as NFκB and small GTPase signal molecules[32, 33]. Efforts towards defining modulators of molecular and genetic predisposition to renal fibrosis suggest a major role for the Notch pathway integration into the TGF-β signaling module [32–35]. Our work presented here and reports by others is building on the hypothesis that Notch receptor proteins, the intracellular domain and respective ligands for these receptors, are responsible in part for exacerbation and progression of chronic kidney diseases typified by renal fibrosis [36]. Notch protein signaling is of particular importance due to their effects on many biological processes. Notch proteins can impart pleiotropic effects in metazoan development, including neural crest development, cell fate determination, tissue patterning, vasculogenesis and morphogenesis [37]. Our biochemical isolation of active Notch4$^{ICD}$ indicates a novel interaction between the Notch4$^{ICD}$ and Elongin C, a component of the E3 ubiquitin ligase complex, and could point towards another node of regulation disrupted in diabetic nephropathy.

Elongin C was originally identified as a protein important in the suppression of pausing by RNA polymerase II during the elongation phase of transcription and has since been found to be a core component of an SCF-related ubiquitin ligase (E3 enzyme) [38]. A number of transcription factors have been implicated as targets of an Elongin C-based ubiquitin ligase including HIF1α [39, 40], c-myc [41], p53 [42, 43] and NF-kB [44]. Our results indicate that

the transcriptionally active domain of Notch4 (Notch4$^{ICD}$) is an Elongin C target, implicating the Elongin C complex in the downregulation of Notch4 signaling. With a known, active presence at sites of transcription, the Elongin C complex could act to quickly terminate Notch4 signaling after it has activated a round of transcription. Such a role in Notch1 signaling has been described for a different E3 that uses the F box protein Fbw7/Sel-10 as the substrate receptor for a cullin-1-based ubiquitin ligase activity [21, 22].

Fbw7/Sel-10 has been shown to bind phosphorylated Notch1$^{ICD}$ and Notch4$^{ICD}$ *in vitro* [22]. However, although Fbw7/Sel-10 over-expression depressed Notch1 activity and protein levels, no effect of Fbw7/Sel-10 over-expression was seen on Notch4 expression or signaling. In contrast, Fbw7/Sel-10 deletion in mice leads to the stabilization of Notch4 in embryo vascular tissues after 10.5 days [45]. Together, these reports suggest that Fbw7/Sel10 functions in Notch4 turnover during development, but not in fully differentiated cells. Thus, perhaps Fbw7/Sel-10 is the primary ubiquitin complex regulating Notch1 and Notch4 in embryonic development, while Elongin C complexes could serve as the primary regulator of Notch4 post-development. Differences in regulation might be expected as Notch4 has diverged considerably from the other mammalian Notch genes [46]. In particular, Notch4 lacks a recognizable transcriptional activation domain between the ankyrin repeats and the PEST sequence at the carboxy terminus and the distance between these two domains is considerably less in Notch4 than in any of its mammalian paralogs. Worth noting, is the fact that different isoforms of Notch have some overlapping functions and features, this could be important in differentiating the functions of Notch4$^{ICD}$ as related to the functions of Notch1$^{ICD}$.

Elongin C complexes could have a role in the dysregulation of Notch4 in epithelial injury and disease. Over-expression of Notch4 protein or mRNA has been implicated in a number of epithelial-derived carcinomas including, malignant melanoma, pancreatic cancer, breast cancer and genital tract cystadenoma and squamous metaplasia [47–50]. We have found that proximal tubule cell expression of Notch4$^{ICD}$ is enhanced in the fibrotic kidneys from diabetic mice and patients. We also show that overexpression of the active Notch4$^{ICD}$ augments TGF-β-directed transcriptional activity and fibrosis in kidney tubule cells and this function is inhibited by co-expression of Elongin C.

Interestingly, in experiments where Elongin C and Notch4$^{ICD}$ were co-expressed in kidney tubule cells, Elongin C levels were noticeably decreased relative to cells only over-expressing Elongin C. This indicates that upon substrate recognition and subsequent ubiquitination, Elongin C may also be targeted for degradation. This type of mechanism has been reported for other ubiquitin ligase components such as Mdm2 [51] and Nedd4-2 [52]. This also suggests a feedback mechanism that could contribute to gain of Notch4 and loss of Elongin C expression and function in diseased epithelial kidney tissue.

Elongin C does not usually function as the substrate receptor but plays a role similar to that of Skp1 in the cullin-1-containing SCF, acting as a linker between the cullin and the substrate receptor [20]. Several candidates for substrate receptor were uncovered in our proteomic screen including MUF1, Elongin A, SOCS5 and SOCS-box containing 7, but none of these appeared with the consistency found for Elongin C. SOCS5 and SOCS-box containing 7 are usually involved in cytosolic events and may be involved in events more closely timed with early steps in Notch4 signaling. MUF1 and elongin A are nuclear and both are excellent candidates for the substrate receptor specific for transcriptionally active Notch4$^{ICD}$. Cullin-5 enrichment was also noted in our proteomic screen. This is significant because, relative to the SCF system, Elongin complexes have an additional level of complexity in that they can be assembled with one of two different cullins, either cullin-2 or cullin-5 [53, 54]. The cullins are the site of attachment for different RING box-containing

proteins, Rbx1 for cullin-2 and Rbx2 for cullin-5, which, in turn, mediate selection of the ubiquitin conjugating enzyme (E2) that actually catalyzes the ubiquitination reaction. The choice of cullin is significant because, in the Elongin complex, the cullin influences the choice of substrate receptor. Cullin-2•Elongin C complexes prefer to interact with the von Hippel-Lindau (Vhl) substrate receptor, while cullin-5•Elongin C complexes prefer to interact with Elongin A, MUF1 and SOCS box-containing substrate receptors, the candidate substrate receptors found in our screens. This is also consistent with Vhl not being detected in our screen. Ongoing studies will define the nature and role(s) of these potential Notch4$^{ICD}$ interactors.

In summary, we examined protein-protein interaction complexes of Notch4$^{ICD}$ to unveil novel molecular interactions and discovered a potentially important interaction with Elongin C. Our follow-up studies indicate a negative regulatory function whereby Elongin C down-regulates Notch4$^{ICD}$ activity in a proteasome dependent manner. Upon examination of Elongin C expression levels in human diabetic kidney sections, we found a marked decrease of Elongin C protein, particularly in the tubule structures which is reciprocally correlated with fibrosis and extracellular matrix deposition. Though we cannot speculate if Elongin C is primarily responsible for ubiquitin mediated degradation of Notch4$^{ICD}$, it is highly likely that this protein is responsible for the regulation of a portion of the Notch4$^{ICD}$ pools post-development in the kidney tubules.

### Highlights

- Notch4$^{ICD}$ acts in concert with TGF-β pathway to drive fibrotic signaling.
- Proteomics studies indicate Notch4$^{ICD}$ and elongin C interact.
- Functional studies show elongin C inhibits Notch4-mediated TGF-β fibrotic activity.
- Elongin C negatively regulates Notch4$^{ICD}$ in a proteasome dependent manner.
- Elongin C is minimally expressed in type 1 diabetic renal proximal tubule cells.

## Acknowledgments

We thank Shirong Zheng for supplying kidney samples from OVE26 mice and Susan Coventry for archived diabetic patient biopsies. This study was supported by funding from the office of Science Financial Assistance Programs, US Department of Energy. D.W.P.was supported by a National Institutes of Health Grant DK176743, Kentucky Diabetes Research Board and Juvenile Diabetes Research Foundation. T.D.C. was supported by American Recovery and Reinvestment Act supplement to DK176743.

## References

1. Androutsellis-Theotokis A, et al. Notch signalling regulates stem cell numbers in vitro and in vivo. Nature. 2006; 442(7104):823–826. [PubMed: 16799564]
2. McCright B. Notch signaling in kidney development. Curr Opin Nephrol Hypertens. 2003; 12(1):5–10. [PubMed: 12496659]
3. Hirsinger E, et al. Notch signalling acts in postmitotic avian myogenic cells to control MyoD activation. Development. 2001; 128(1):107–116. [PubMed: 11092816]
4. Anderson LM, Gibbons GH. Notch: a mastermind of vascular morphogenesis. J Clin Invest. 2007; 117(2):299–302. [PubMed: 17273550]
5. Olivier A, et al. The Notch ligand delta-1 is a hematopoietic development cofactor for plasmacytoid dendritic cells. Blood. 2006; 107(7):2694–2701. [PubMed: 16357328]

6. Pourquie O. Skin development: delta laid bare. Curr Biol. 2000; 10(11):R425–R428. [PubMed: 10837237]
7. Fleming RJ. Structural conservation of Notch receptors and ligands. Semin Cell Dev Biol. 1998; 9(6):599–607. [PubMed: 9918871]
8. Kopan R. Notch: a membrane-bound transcription factor. J Cell Sci. 2002; 115(Pt 6):1095–1097. [PubMed: 11884509]
9. Baron M. An overview of the Notch signalling pathway. Semin Cell Dev Biol. 2003; 14(2):113–119. [PubMed: 12651094]
10. Schweisguth F. Regulation of notch signaling activity. Curr Biol. 2004; 14(3):R129–R138. [PubMed: 14986688]
11. Nath KA. Tubulointerstitial changes as a major determinant in the progression of renal damage. Am J Kidney Dis. 1992; 20(1):1–17. [PubMed: 1621674]
12. Nath KA. The tubulointerstitium in progressive renal disease. Kidney Int. 1998; 54(3):992–454. [PubMed: 9734628]
13. Bottinger EP, Bitzer M. TGF-beta signaling in renal disease. J Am Soc Nephrol. 2002; 13(10): 2600–2610. [PubMed: 12239251]
14. Quillard T, et al. Impaired Notch4 activity elicits endothelial cell activation and apoptosis: implication for transplant arteriosclerosis. Arterioscler Thromb Vasc Biol. 2008; 28(12):2258–2265. [PubMed: 18802018]
15. Sun Y, et al. Notch4 intracellular domain binding to Smad3 and inhibition of the TGF-beta signaling. Oncogene. 2005; 24(34):5365–5374. [PubMed: 16007227]
16. Tang Y, et al. Notch and transforming growth factor-beta (TGFbeta) signaling pathways cooperatively regulate vascular smooth muscle cell differentiation. J Biol Chem. 2010; 285(23): 17556–17563. [PubMed: 20368328]
17. Harreman M, et al. Distinct ubiquitin ligases act sequentially for RNA polymerase II polyubiquitylation. Proc Natl Acad Sci U S A. 2009
18. Yasukawa T, et al. Mammalian Elongin A complex mediates DNA-damage-induced ubiquitylation and degradation of Rpb1. EMBO J. 2008; 27(24):3256–3266. [PubMed: 19037258]
19. Gerber M, et al. In vivo requirement of the RNA polymerase II elongation factor elongin A for proper gene expression and development. Mol Cell Biol. 2004; 24(22):9911–9919. [PubMed: 15509793]
20. Willems AR, Schwab M, Tyers M. A hitchhiker's guide to the cullin ubiquitin ligases: SCF and its kin. Biochim Biophys Acta. 2004; 1695(1–3):133–170. [PubMed: 15571813]
21. Fryer CJ, White JB, Jones KA. Mastermind recruits CycC:CDK8 to phosphorylate the Notch ICD and coordinate activation with turnover. Mol Cell. 2004; 16(4):509–520. [PubMed: 15546612]
22. Wu G, et al. SEL-10 is an inhibitor of notch signaling that targets notch for ubiquitin-mediated protein degradation. Mol Cell Biol. 2001; 21(21):7403–7415. [PubMed: 11585921]
23. Koncarevic A, Jackman RW, Kandarian SC. The ubiquitin-protein ligase Nedd4 targets Notch1 in skeletal muscle and distinguishes the subset of atrophies caused by reduced muscle tension. FASEB J. 2007; 21(2):427–437. [PubMed: 17172638]
24. Nie L, et al. Notch-induced Asb2 expression promotes protein ubiquitination by forming noncanonical E3 ligase complexes. Cell Res. 2011; 21(5):754–769. [PubMed: 21119685]
25. Heuze ML, et al. ASB2 is an Elongin BC-interacting protein that can assemble with Cullin 5 and Rbx1 to reconstitute an E3 ubiquitin ligase complex. J Biol Chem. 2005; 280(7):5468–5474. [PubMed: 15590664]
26. Gingras AC, et al. A novel, evolutionarily conserved protein phosphatase complex involved in cisplatin sensitivity. Mol Cell Proteomics. 2005; 4(11):1725–1740. [PubMed: 16085932]
27. Cummins TD, et al. Quantitative mass spectrometry of diabetic kidney tubules identifies GRAP as a novel regulator of TGF-beta signaling. Biochim Biophys Acta. 2009
28. Keller A, et al. Empirical statistical model to estimate the accuracy of peptide identifications made by MS/MS and database search. Anal Chem. 2002; 74(20):5383–5392. [PubMed: 12403597]
29. Nesvizhskii AI, et al. A statistical model for identifying proteins by tandem mass spectrometry. Anal Chem. 2003; 75(17):4646–4658. [PubMed: 14632076]

30. Jiang X, Sorkin A. Coordinated traffic of Grb2 and Ras during epidermal growth factor receptor endocytosis visualized in living cells. Mol Biol Cell. 2002; 13(5):1522–1535. [PubMed: 12006650]

31. Uyttendaele H, et al. Notch4/int-3, a mammary proto-oncogene, is an endothelial cell-specific mammalian Notch gene. Development. 1996; 122(7):2251–2259. [PubMed: 8681805]

32. Nyhan KC, et al. Jagged/Notch signalling is required for a subset of TGFbeta1 responses in human kidney epithelial cells. Biochim Biophys Acta. 1803(12):1386–1395. [PubMed: 20833210]

33. Zavadil J, et al. Integration of TGF-beta/Smad and Jagged1/Notch signalling in epithelial-to-mesenchymal transition. Embo J. 2004; 23(5):1155–1165. [PubMed: 14976548]

34. Bielesz B, et al. Epithelial Notch signaling regulates interstitial fibrosis development in the kidneys of mice and humans. J Clin Invest. 120(11):4040–4054. [PubMed: 20978353]

35. Niranjan T, et al. The Notch pathway in podocytes plays a role in the development of glomerular disease. Nat Med. 2008; 14(3):290–298. [PubMed: 18311147]

36. Sharma S, Sirin Y, Susztak K. The story of Notch and chronic kidney disease. Curr Opin Nephrol Hypertens. 2011; 20(1):56–61. [PubMed: 21088575]

37. Heitzler P. Biodiversity and noncanonical Notch signaling. Curr Top Dev Biol. 2010; 92:457–481. [PubMed: 20816404]

38. Iwai K, et al. Identification of the von Hippel-lindau tumor-suppressor protein as part of an active E3 ubiquitin ligase complex. Proc Natl Acad Sci U S A. 1999; 96(22):12436–12441. [PubMed: 10535940]

39. Lonergan KM, et al. Regulation of hypoxia-inducible mRNAs by the von Hippel-Lindau tumor suppressor protein requires binding to complexes containing elongins B/C and Cul2. Mol Cell Biol. 1998; 18(2):732–741. [PubMed: 9447969]

40. Ohh M, et al. Ubiquitination of hypoxia-inducible factor requires direct binding to the betadomain of the von Hippel-Lindau protein. Nat Cell Biol. 2000; 2(7):423–427. [PubMed: 10878807]

41. Kimura Y, et al. MM-1 facilitates degradation of c-Myc by recruiting proteasome and a novel ubiquitin E3 ligase. Int J Oncol. 2007; 31(4):829–836. [PubMed: 17786314]

42. Luo K, et al. Adenovirus E4orf6 assembles with Cullin5-ElonginB-ElonginC E3 ubiquitin ligase through an HIV/SIV Vif-like BC-box to regulate p53. Faseb J. 2007; 21(8):1742–1750. [PubMed: 17351129]

43. Cai QL, et al. EC5S ubiquitin complex is recruited by KSHV latent antigen LANA for degradation of the VHL and p53 tumor suppressors. PLoS Pathog. 2006; 2(10):e116. [PubMed: 17069461]

44. Maine GN, et al. COMMD1 promotes the ubiquitination of NF-kappaB subunits through a cullincontaining ubiquitin ligase. Embo J. 2007; 26(2):436–447. [PubMed: 17183367]

45. Tsunematsu R, et al. Mouse Fbw7/Sel-10/Cdc4 is required for notch degradation during vascular development. J Biol Chem. 2004; 279(10):9417–9423. [PubMed: 14672936]

46. Theodosiou A, et al. Evolutionary scenarios of Notch proteins. Mol Biol Evol. 2009; 26(7):1631–1640. [PubMed: 19369596]

47. Frew IJ, et al. Combined VHLH and PTEN mutation causes genital tract cystadenoma and squamous metaplasia. Mol Cell Biol. 2008; 28(14):4536–4548. [PubMed: 18474617]

48. Miyamoto Y, et al. Notch mediates TGF alpha-induced changes in epithelial differentiation during pancreatic tumorigenesis. Cancer Cell. 2003; 3(6):565–576. [PubMed: 12842085]

49. Nickoloff BJ, Osborne BA, Miele L. Notch signaling as a therapeutic target in cancer: a new approach to the development of cell fate modifying agents. Oncogene. 2003; 22(42):6598–6608. [PubMed: 14528285]

50. Callahan R, Egan SE. Notch signaling in mammary development and oncogenesis. J Mammary Gland Biol Neoplasia. 2004; 9(2):145–163. [PubMed: 15300010]

51. Fang S, et al. Mdm2 is a RING finger-dependent ubiquitin protein ligase for itself and p53. J Biol Chem. 2000; 275(12):8945–8951. [PubMed: 10722742]

52. Bruce MC, et al. Regulation of Nedd4-2 self-ubiquitination and stability by a PY motif located within its HECT-domain. Biochem J. 2008; 415(1):155–163. [PubMed: 18498246]

53. Brower CS, et al. Mammalian mediator subunit mMED8 is an Elongin BC-interacting protein that can assemble with Cul2 and Rbx1 to reconstitute a ubiquitin ligase. Proc Natl Acad Sci U S A. 2002; 99(16):10353–10358. [PubMed: 12149480]

54. Mahrour N, et al. Characterization of Cullin-box sequences that direct recruitment of Cul2-Rbx1 and Cul5-Rbx2 modules to Elongin BC-based ubiquitin ligases. J Biol Chem. 2008; 283(12): 8005–8013. [PubMed: 18187417]

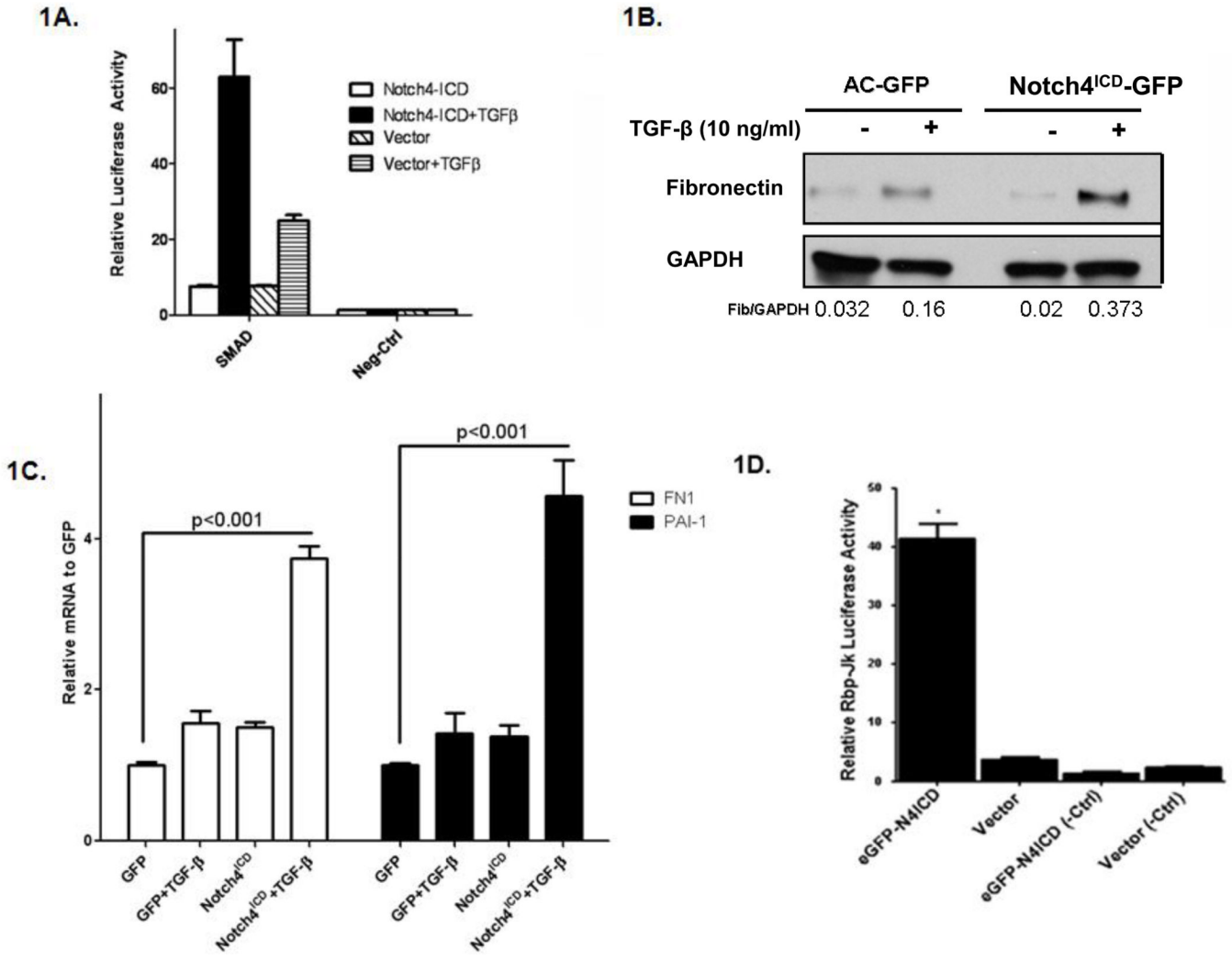


**Figure 1. Notch4$^{ICD}$ regulates TGF-β activity**

**A.** Luciferase activity was measured following co-transfection of HK11 cells with a TGF-β-responsive SMAD2/3/4 reporter and Notch4$^{ICD}$-GFP or GFP control constructs +/− TGF-β1 (10 ng/ml) stimulation or with a luciferase construct lacking the responsive element (Neg-Ctrl). Columns are the mean of 3 biological replicates and the error bars are +/− SEM. Notch4$^{ICD}$ potentiated SMAD-luciferase activity in the presence of TGF-β ~3-fold over TGF-β alone. **B.** Immunoblot analysis of fibronectin and GAPDH (loading control) following treatment of HK11 cells +/− recombinant TGF-β1 and transfection with Notch4$^{ICD}$-GFP or GFP vector control. Cells were transfected overnight and then treated with TGF-β (10 ng/ml) for 24 hours. **C.** Quantitative real time RT-PCR of fibronectin and PAI-1 levels in HK11 cells transfected with Notch4$^{ICD}$-GFP or GFP +/− TGF-β stimulation. 18S rRNA was used to normalize fibronectin signal. **D.** Activity of Notch4$^{ICD}$-GFP construct was confirmed using an Rbp-Jk luciferase reporter specific for Notch activity. Fold increase is relative to GFP (vector) only transfected cells. Columns are mean of 3 biological replicates and the error bars are +/− SEM.

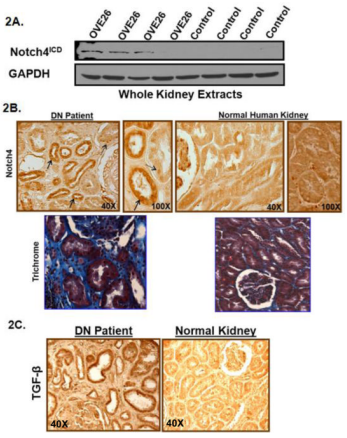


**Figure 2. Notch4$^{ICD}$ levels are elevated in fibrotic kidney tissue**

**A.** Lysates from whole kidneys of type 1 diabetic mice (OVE26) were examined by immunoblot to determine levels of Notch4$^{ICD}$. **B**. Human biopsies from type 1 diabetic nephropathy (DN) patients exhibiting fibrosis (trichrome stain) were analyzed by immunohistochemistry (IHC). IHC from a representative sample shows enhanced Notch4$^{ICD}$ levels in diffuse cellular (solid arrows) and some nuclear regions (dashed arrows). Nuclear Notch4 staining would indicate potential transcriptional activity in these areas. **C.** IHC indicating elevated TGF-β signaling. Consistent results were observed with comparison of kidney biopsy sections from 3 type 1 diabetic nephropathy patients and 3 normal individuals.

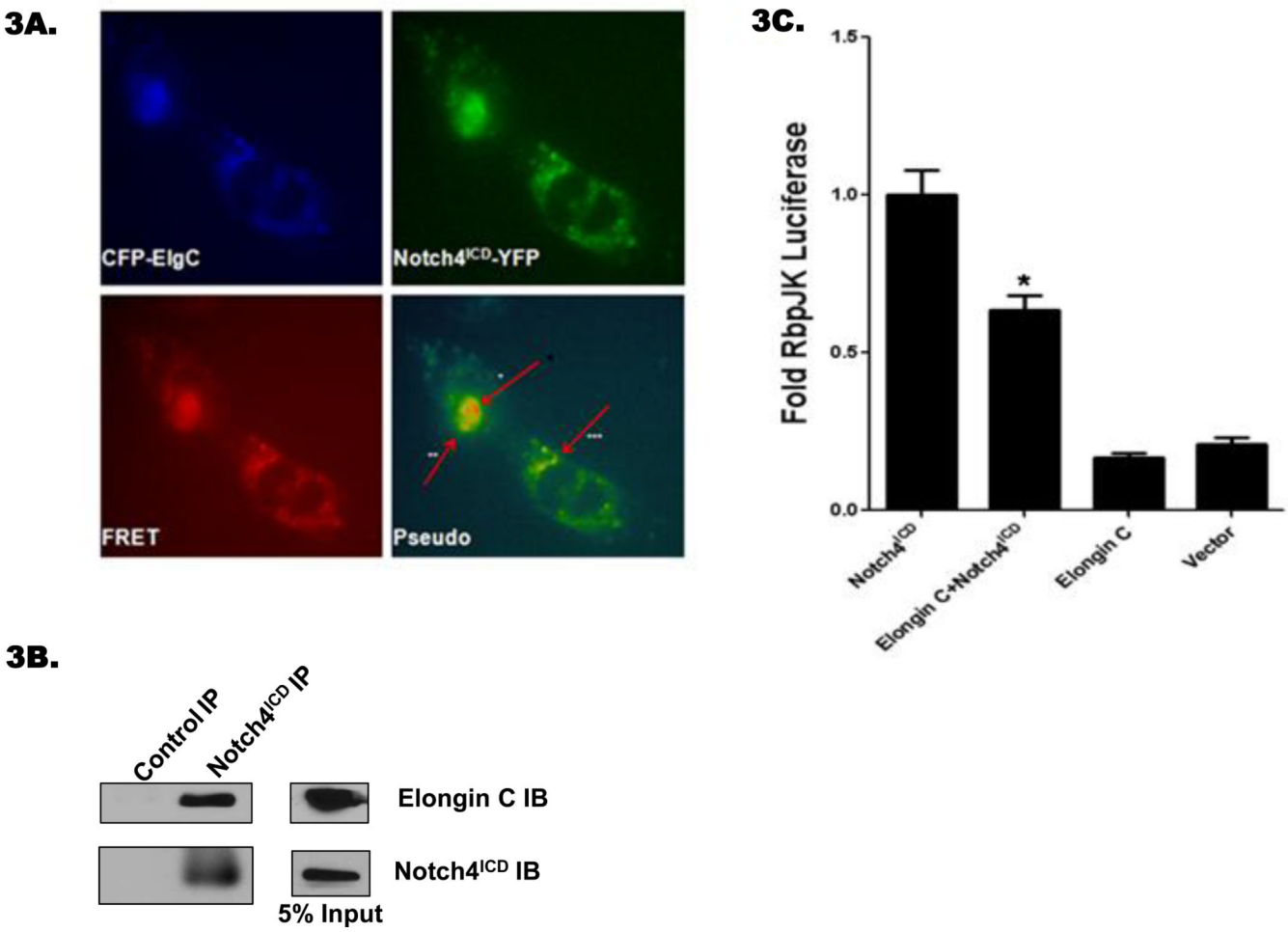


**Figure 3. Elongin C regulates Notch4$^{ICD}$ function**

**A.** Notch4$^{ICD}$ and Elongin C interaction was validated by FRET analysis in HK11 cells ectopically expressing CFP-tagged Elongin C (Upper left) and YFP-tagged Notch4$^{ICD}$ (upper right). FRET is indicated in red (lower left) while Pseudo (lower right). Panels show CFP, YFP excitation and FRET donor excitation. The red/orange areas in the pseudo colored image labeled FRET represent positive interactions. Pearson correlation coefficients were calculated where > 0.8 is indicated by an arrow. Both nuclear and cytoplasmic interaction was indicated. B. Immunoblot (IB) for Elg C and Notch$^{ICD}$ shows that native Elg C co-purified with native Notch4$^{ICD}$ immuno-purification (IP), but not control purification from HK11 lysate (1 mg). **C.** HK11 cells were transfected with Notch4$^{ICD}$ and Elongin C at equal amounts along with a Notch-responsive Rbp-jk reporter and renilla luciferase constructs to determine effect of Elongin C on Notch4$^{ICD}$ transcription activity. In replicate assays the presence of Elongin C caused a 40% reduction in reporter activity. Columns are mean of 3 biological replicates and the error bars are +/− SEM.

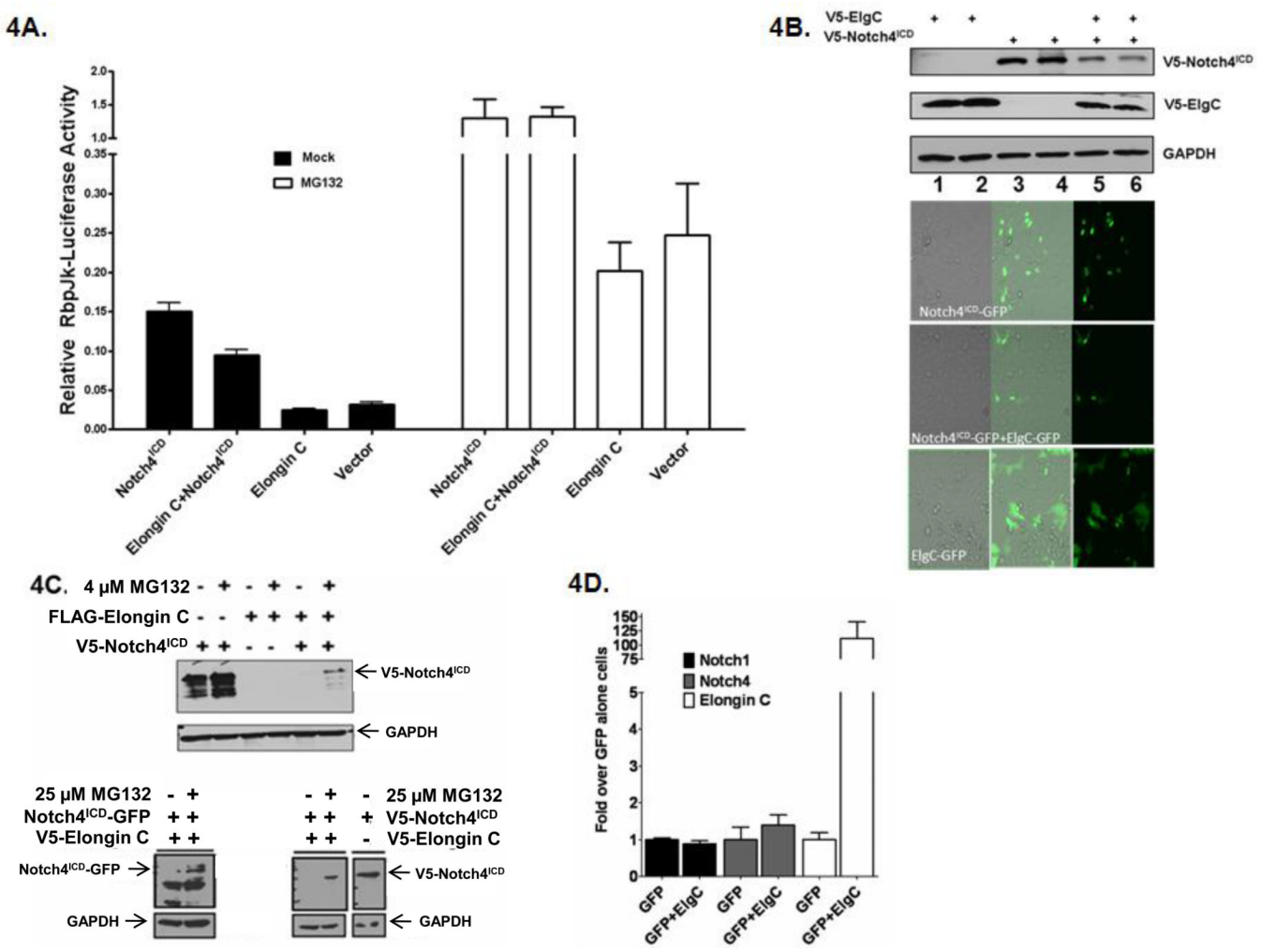


**Figure 4. Elongin C regulates Notch4$^{ICD}$ activity and protein level via a proteasome mechanism**

**A.** Luciferase activity was determined following transfection of HK11 cells with a Notch-responsive Rbp-jk reporter and control vector, Notch4$^{ICD}$, Elongin C, or Notch4$^{ICD}$ and Elongin C constructs together with (black bars) or without (white bars) pre-treatment with MG132 proteasome inhibitor. Columns are mean of 3 biological replicates and the error bars are +/− SEM. **B.** Upper panel shows HK11 cell cultures transfected in duplicate with either V5-Elongin C (lanes 1 and 2), V5-Notch4$^{ICD}$ (lanes 3 and 4), or V5-Notch4$^{ICD}$ and V5-Elongin C (lanes 5 and 6). Following 24-hour transfection, cell lysates were immunoblotted for V5 and GAPDH (loading control). Lower panel shows confocal microscopy images of either Notch4$^{ICD}$-GFP, Notch4$^{ICD}$-GFP and ElgC-GFP, or ElgC-GFP transfected HK11 cells. These are representative images of more than 3 biological replicates. **C.** HK11 cells were pretreated with 4 μM MG132 for 4 hours before transfection with either V5-Notch4$^{ICD}$ +/− Flag-Elongin C or Flag-Elongin C alone (upper panel). Lower panel shows similar experiment with increased MG132 (25 μM) pretreatment followed by transfection with GFP-Notch4$^{ICD}$ +/− V5-Elongin C or V5-Notch4$^{ICD}$ +/− V5-Elongin C (right panel). **D.** Shows quantitative RT-PCR using primers for Notch 1 (black bars), Notch4 (gray bars), or Elongin C (white bars) following transfection of HK11 with GFP-Elongin C or GFP as the control condition, data represent means and n=3 biological replicates, error bars are +/−SEM.

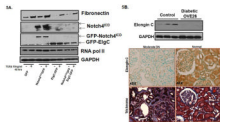

**Figure 5. Elongin C regulates Notch4$^{ICD}$-mediated TGF-β activity**

**A.** Immunoblot analysis for fibronectin, Notch4$^{ICD}$, GFP, RNA polymerase (pol) II, and GAPDH (loading control) following treatment of HK11 cells with and without recombinant TGF-β1 and transfections with GFP- Notch4$^{ICD}$, GFP control, or GFP-Notch4$^{ICD}$ and GFP-Elongin C. Cells were transfected overnight and then treated with TGF-β (10 ng/ml) for 48 hours. **B.** Elongin C protein levels were measured in type 1 diabetic mouse tubule extracts and control strain extracts by immunoblot (left panel). Immunohistochemistry (IHC) showing diminished renal tubule Elongin C levels in biopsies from a type 1 diabetic human kidney. Trichrome staining indicates moderate fibrotic scarring in the diabetic kidney. Elongin C IHC shown are representative results that were consistently observed comparisons of kidneys from 3 type 1 diabetic nephropathy patients and 3 normal individuals.

## Table 1.

| Protein Name | Accession # | Replicate Purification | Average PAF |
|---|---|---|---|
| Elongin C (TCEB1) | AAl00029.1 | 4 of 4 | 1.2 |
| SKp1 | NP_733779.1 | 2 of 4 | 0.54 |
| MUF1 (Elongin C Binding) | Q15345.3 | 2 of 4 | 0.26 |
| Elongin A | AAA75492.1 | 1 of 4 | 0.12 |
| Elongin A Binding Protein | NP_003186.1 | 2 of 4 | 0.08 |
| SOCS5 | NP_659198.1 | 2 of 4 | 0.16 |
| SOCS Box Containing 7 | NP_078984.2 | 2 of 4 | 0.33 |
| Cullin 5 | AAK07472.1 | 2 of 4 | 0.21 |
| Nedd8-Conjugating Enzyme | NP_542409.1 | 1 of 4 | 0.5 |
| CDK7 (Homolog) | EAW51301.1 | 2 of 4 | 0.26 |